Journal of Catalysis **182,** 48–55 (1999)
Article ID jcat.1998.2304, available online at http://www.idealibrary.com on IDEAL®

Platinum-Oxide Species Formed on Progressive Oxidation of Platinum Crystallites Supported on Silica and Silica–Alumina

Chin-Pei Hwang and Chuin-Tih Yeh[1]

Department of Chemistry, National Tsing-Hua University, Hsinchu, 30043, Taiwan, Republic of China

Received April 21, 1998; revised October 2, 1998; accepted October 19, 1998

Samples of platinum crystallites finely dispersed on silica and silica–alumina were prepared by impregnating a series of SiO_2–Al_2O_3 supports with aqueous $PtCl_4$ solutions. Reduced platinum samples were oxidized by dioxygen to examine variations of platinum-oxides (Pt-O_x) species formed with the oxidation temperature (T_O). Both PtO and PtO_2 species were verified to coexist on oxidized Pt/SiO_2 samples according to characterizations by techniques of X-ray photoelectron spectroscopy and temperature-programmed reduction (TPR). TPR spectra of oxidized platinum species dispersed on SiO_2–Al_2O_3 supports exhibited six peaks of different reduction temperatures (T_r). These peaks were assigned to PtO and PtO_2 species dispersed in silica-rich grains ($T_r = -40$ and 20°C, respectively), in alumina-rich grains ($T_r = 50$ and 90°C), and in pores of the grain boundary ($T_r = 110$ and 130°C), respectively. The contribution of these six species varied with both the temperature of oxidation treatments and the Al_2O_3/SiO_2 ratio of sample supports.

1. INTRODUCTION

Supported platinum catalysts are currently used in reactions of the catalytic combustion (1–3) and the partial oxidation (4–6). During these catalytic reactions, the surface platinum atoms on dispersed crystallites are reversibly changed between the oxidized state and the metallic state; i.e.,

$$Pt \underset{RH}{\overset{O_2}{\Longleftrightarrow}} 2\,PtO_x. \qquad [1]$$

In this equation, x and RH denote a chemical stoichiometry of platinum oxides and reductive molecules in catalytic systems, respectively.

The oxidation of supported platinum crystallites has been widely studied in the literature. A severe oxidation not only induced a change in their size distribution and morphology (7–14), but also generated platinum oxides of different stoichiometries (7, 14–25). In a recent TPR (temperature-programmed reduction) study (21) on oxidation of Pt/Al_2O_3 samples, oxidized platinum ions in four different environments, i.e., chemisorbed (PtO^c), PtO, PtO_2, and $PtAl_2O_4$, have been distinguished from their reduction temperatures in TPR traces. The relative contribution of these four species on oxidized samples varied significantly with the platinum dispersion and the oxidation temperature.

The support of catalysts generally has a prominent effect on behavior of dispersed active ingredients. Both the morphology and the reducibility of molybdenum oxides dispersed on SiO_2–Al_2O_3 were significantly affected by the support composition (26, 27). It becomes a pertinent topic to study "Whether the support can affect the oxidation of dispersed platinum." In the literature, different platinum-oxide species [PtO (14, 25) or PtO_2 (24)] have been suggested as probable platinum oxide species on silica supported Pt/SiO_2 samples calcined at a temperature of 300°C (Table 1).

In this study, platinum oxide species formed on oxidation of a series of Pt/SiO_2–Al_2O_3 samples with different SiO_2/Al_2O_3 ratios in support composition were investigated with the established TPR technique. We want to report that the composition of supports also has a profound effect on the reductive properties of platinum oxides formed.

2. EXPERIMENTAL

2.1. Fresh and Reduced Pt/SiO_2 Samples

Pt/SiO_2 samples of different platinum loadings were prepared by impregnating SiO_2 powders (Carbosil M-5, surface area 200 $m^2\,g^{-1}$) with aqueous $PtCl_4$ solutions by the incipient-wetness method. Obtained slurries were subsequently dried overnight at 110°C, calcined for 4 h at 300°C and stored as fresh samples. A major portion of each fresh sample was then reduced by flowing hydrogen for 2 h at 300°C to convert supported PtO_xCl_y into chloride-free Pt crystallites (7, 21) and is described in this paper as the reduced sample.

[1] To whom correspondence should be addressed. Fax: 886-3-5711082. E-mail: ctyeh@chem.nthu.edu.tw.

0021-9517/99 $30.00

TABLE 1

TPR Characterization of Silica Supported Platinum Oxide Species Suggested in Literature

Authors	Sample	Oxidation condition	TPR		Oxide species	Ref.
			T_r (°C)	N_O/N_{Pt}		
Bond *et al.*	6.3% Pt/SiO_2 (EUROPT-1)	TPO upward to 300°C	−60 and 20	0.9	PtO	14
Sachtler *et al.*	Pt/SiO_2	300°C oxidation	−15 and 30	0.95	PtO	25
Maccabe *et al.*	0.7 and 5.2% Pt/SiO_2	300°C oxidation	−70–130	2 (assumed)	PtO_2	24
This study	1.0 and 4.9% Pt/SiO_2	25–600°C oxidation	−50 and 20	0.23–1.21	PtO and PtO_2	

2.2. Pt/SiO_2–Al_2O_3 Samples

Three kinds of commercial silica–alumina powders from Wako Co. were used as the starting supports. Their SiO_2/Al_2O_3 weight ratios were 80/20 (hereafter named as SA-80), 75/25 (SA-75), and 40/60 (SA-40), respectively. Supported Pt/SiO_2–Al_2O_3 samples with a nominal platinum loading of 5 wt% were prepared by impregnating the SiO_2–Al_2O_3 powders with a $PtCl_4$ solution. The impregnated samples were pretreated with an overnight drying at 110°C and a 4-h calcination at 300°C. These fresh samples were subsequently reduced for 2 h at 300°C, and named as reduced Pt/SA-80, Pt/SA-75, and Pt/SA-40, respectively.

2.3. Oxidized Samples

Each reduced sample (Pt/SiO_2 or Pt/SiO_2-Al_2O_3) was divided into several portions. They were oxidized in a gaseous flow of 5 vol% O_2 in He for 2 h at different predetermined oxidation temperatures ($T_O = -100$, −40, 25, 100, 300, 400, 500, or 600°C) to convert supported platinum crystallites into oxidized states. Variations in the platinum loading and the oxidation state of platinum on these oxidized samples were characterized by ICP and TPR techniques.

2.4. ICP Measurements

Loadings of platinum on reduced samples were analyzed by a Perkin-Elemer Sciex Elan 5000 ICP-MS. Each sample was pretreated with a 2-h dehydration at 200°C and a complete dissolution in aqua regia. Measured platinum loading on Pt/SiO_2 samples decreased with the temperature of oxidation treatments when $T_O > 400$°C (Table 2), probably due to an increased extent of the following sublimation reaction (9, 28):

$$Pt + O_2 = PtO_{2(g)}. \quad [1]$$

2.5. TPR Characterizations

TPR studies were performed in a fixed bed apparatus described in the previous report (29). A 30 ml min^{-1} flow

TABLE 2

Effects of Oxidation Temperature (T_O) on Pt Loadings and the TPR Characterization of Silica Supported Platinum Samples

Sample (Dispersion $D = N_H/N^s_{Pt}$)[a]	T_O (°C)	ICP/MS (Pt wt%)	TPR peak (area %)		Total peak area, H_2 consumption in TPR (10^{-5} mol)	N_O/N_{Pt}[b]
			$T_r = -50$°C (S_1)	$T_r = 20$°C (S_2)		
4.9% Pt/SiO_2	−100	—	100	0	0.85	0.23
($D = 30\%$)	−40	—	100	0	1.52	0.41
	25	4.9	95	5	2.77	0.74
	100	4.9	88	12	3.67	0.98
	300	4.8	75	25	3.83	1.03
	400	4.0	70	30	3.76	1.21
	500	3.9	80	20	3.32	1.10
	600	3.4	85	15	2.60	0.99
1.0% Pt/SiO_2	25	—	90	10	0.69	0.91
($D = 50\%$)	300	1.0	75	25	0.92	1.19
	500	0.9	70	30	0.96	1.25

[a] N_H, monolayer uptake of hydrogen atom from H_2 chemisorption at 25°C. Assuming that $N_H/N^s_{Pt} = 1.1$ (29).
[b] N_{Pt}, number of platinum atom measured from ICP/MS.
N_O, uptake of oxygen atom calculated from H_2 consumption in TPR.

TABLE 3

Reduction Temperature (T_r) in TPR for Various Platinum Oxide Species Formed on γ-Al_2O_3 and SiO_2 Supports

Oxide species	T_r (°C)	
	Pt/Al_2O_3[a]	Pt/SiO_2[b]
Bulk PtO_xCl_y	150–300	~60
Intersurfacial PtO_xCl_y	300–400	~100
Pt^sO	−25	−60
PtO	50	−50
PtO_2	100	20
Pt-aluminate	220	—
Pt-silicate	—	None

[a] The data were collected from Ref. 21 in our previous study.
[b] In this study.

of 10 vol% H_2 in Ar was used as the reducing gas when the sample temperature was raised from −80 to 400°C at a constant rate of 7°C min^{-1}. The rate of hydrogen consumption during sample reductions was monitored by a thermal conductivity detector (TCD). The amount of oxygen atoms (N_O) reduced in TPR experiments was measured from the integrated hydrogen consumption. Calculated N_O/N_{Pt} ratios (where N_{Pt} denotes the number of platinum atoms in each sample) from different oxidized samples are listed in Tables 2 and 4. The software used for peak integration was provided by Scientific Information Service Corporation (SISC).

2.6. Hydrogen Chemisorption

Dispersions (D) of platinum on reduced Pt/SiO_2 and Pt/SiO_2–Al_2O_3 samples were estimated by the hydrogen chemisorption measurements performed at room temperature under an assumption that $N_H/N^s_{Pt} = 1.1$ (30) at the monolayer chemisorption. Prior to the chemisorption measurements, reduced samples were pretreated with an evacuation at 300°C for 1 h. The chemisorption was performed volumetrically in a vacuum system described in a previous study (29). Obtained dispersions of platinum on reduced samples are listed in Tables 2 and 4.

TABLE 4

Effect of Oxidation Temperature (T_O) on the TPR Characterization of Pt/SiO_2-Al_2O_3 Samples

Sample Dispersion, D	ICP/MS (Pt/wt%)	N_O/N_{Pt}[a] ratio after varied T_O of oxidation					
		T_O (°C) = 25	100	300	400	500	600
Pt/SA-80 (D = 59%)	4.81	0.46	0.83	1.25	1.26	1.16	0.43
Pt/SA-75 (D = 51%)	4.88	0.69	1.01	1.29	1.32	1.39	0.62
Pt/SA-40 (D = 71%)	4.76	0.74	1.03	1.36	1.49	1.41	0.66

[a] N_{Pt}, number of platinum atom measured from ICP/MS for fresh samples.
N_O, uptake of oxygen atom calculated from H_2 consumption in TPR.

2.7. XPS Characterizations

X-ray photoelectron spectra were obtained from a Perkin-Elmer PHI 1600 Spectrometer using a monochromatic Mg$K\alpha$ X-ray radiation ($h\nu = 15$ keV) at a power of 250 W. The Si 2p peak (103.4 eV) of SiO_2 (31) was used as an internal standard to calibrate the binding energy of peaks in obtained spectra.

2.8. ^{27}Al NMR Characterizations

^{27}Al NMR spectra of silica–alumina supports were obtained from a Bruker MSL-200 spectrometer at an operating frequency of 39.73 MHz. A 3000-Hz magic angle spinning was performed during the signal collection. Reported chemical shifts were related to a standard peak of $Al(H_2O)^{+3}_6$.

3. RESULTS AND DISCUSSION

3.1. Effects of Chloride Ions on Fresh Pt/SiO_2 Samples

Figure 1 displays TPR traces from three fresh Pt/SiO_2 samples of different Pt loadings. The Pt species on these samples may be regarded as PtO_xCl_y complexes (15, 21) because they were prepared from $PtCl_4$ precursor and calcined mildly at 300°C. The two reduction peaks observed

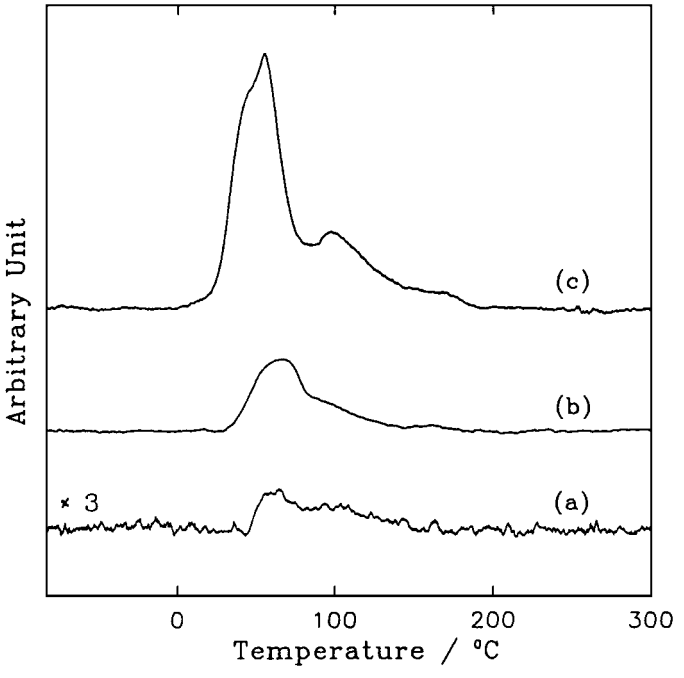

FIG. 1. TPR spectra for reduction of PtO_xCl_y species on fresh Pt/SiO_2 samples. (a) 0.2% Pt/SiO_2, (b) 1.0% Pt/SiO_2, (c) 4.9% Pt/SiO_2.

in Fig. 1 confirmed the literature suggestion (15) that two kinds of PtO_xCl_y complexes, a bulk phase and a dispersive phase, coexisted on fresh platinum samples. The 4.9% Pt/SiO_2 sample consisted mainly of bulk PtO_xCl_y which displayed a TPR peak at $T_r \sim 60°C$. The dispersive phase of PtO_xCl_y interacted substantially with SiO_2 support and exhibited a $T_r \sim 100°C$.

Coordinated chloride ions in the PtO_xCl_y complexes should be removed from platinum by TPR reduction (15, 21) through reactions of

$$PtO_xCl_y + (x + y/2)\,H_2 \rightarrow Pt + x\,H_2O + y\,HCl_{(g)}. \quad [2]$$

Part of the $HCl_{(g)}$ produced may be readsorbed by the silica support and remained on the reduced samples.

3.2. *Effects of Oxidation Treatments on Reduced Pt/SiO_2 Samples*

Figure 2 shows a series of TPR characterizations for eight portions of a reduced 4.9% Pt/SiO_2 sample oxidized at different T_O temperatures. The oxidation reaction may be described by an equation of

$$2\,Pt + x\,O_2 \rightarrow 2\,PtO_x. \quad [3]$$

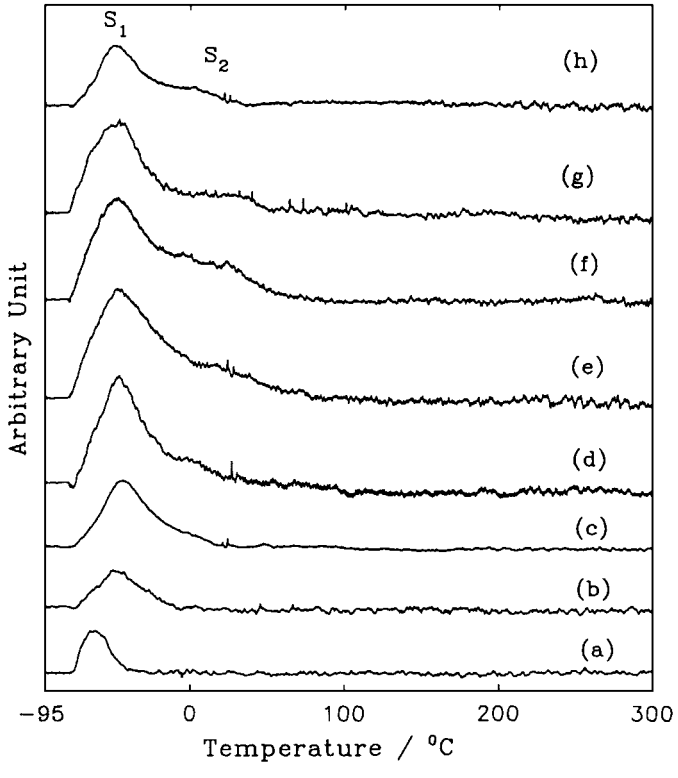

FIG. 2. TPR spectra of oxidized 4.9% Pt/SiO_2 samples which have been pretreated with a 2-h reduction in a flowing hydrogen at 300°C and a subsequent oxidation with 5% oxygen in He at T_0 = (a) −10°C, (b) −40°C, (c) 25°C, (d) 100°C, (e) 300°C, (f) 400°C, (g) 500°C, and (h) 600°C.

Observed reduction temperatures for PtO_x species formed on oxidized samples are always lower than 30°C. A comparison of these TPR traces with those in Fig. 1 reveals that PtO_x species formed on oxidized samples exhibit reduction temperatures lower than that of PtO_xCl_y complexes. The coordinated chloride ions on PtO_xCl_y complexes can, indeed, be removed from platinum upon the prereduction treatment of Eq. [2].

TPR traces in Fig. 2 exhibited two dominant reduction peaks, i.e., S_1 ($T_r = -50°C$) and S_2 ($T_r = 20°C$). Both Bond *et al.* (14) and Sachtler *et al.* (25) also noticed two reduction peaks with similar T_r temperatures from their Pt/SiO_2 samples oxidized at 300°C (Table 1). They reported that the platinum oxide formed on the oxidation had a stoichiometry of $PtO_{0.9}$. The observation of two reduction peaks in a reductive trace indicated that Pt oxides on the oxidized Pt/SiO_2 samples should have stayed in two different chemical environments. Sachtler *et al.* attributed their two peaks to reductions of PtO particles with different sizes. Bond *et al.*, however, suggested that two different morphologies of Pt oxides, i.e., a disordered nonstoichiometric PtO_x (with $T_r = -60°C$) and a stoichiometric PtO (with $T_r = 20°C$), coexisted on the EUROPT-1 catalysts. The assignment of these two reproducible peaks therefore remained in controversy.

In this study, both the relative area and the total area of S_1 and S_2 peaks in TPR traces were found to vary with the temperature T_O of the oxidation pretreatment (Table 2). Trace (a) of Fig. 2 indicates only a narrow peak at $T_r = -60°C$ with a N_O/N_{Pt} ratio = 0.23 after a −100°C oxidation treatment. This low uptake stoichiometry suggests that the oxygen uptake might be limited to a chemisorption of platinum atoms (Pt^s) exposed on the surface of Pt crystallites; i.e.,

$$2\,Pt^s + O_2 \rightarrow 2\,Pt^sO. \quad [4]$$

The extent of oxidation should increase with the oxidation temperature and extend to sublayers of platinum crystallites on raising the T_O temperature from −100 to 100°C. As a result, calculated N_O/N_{Pt} ratio gradually increased upward to 1.0 (traces b–d). Accordingly, the dominant species S_1 formed at $T_O = 100°C$ is therefore assigned to the PtO structure formed from the following oxidation:

$$2\,Pt + O_2 \rightarrow 2\,PtO. \quad [5]$$

Surprisingly, the N_O/N_{Pt} ratio surpassed significantly the expected stoichiometry of 1.0 for PtO and a shoulder peak (S_2) became evident when T_O temperature was raised over to 300°C (traces e–g). Through peak decomposition, areas of the merged S_1 and S_2 peaks in the traces of Fig. 2 were estimated and listed in Table 2. The calculated S_2/S_1 ratio of these traces also increased with the oxidation temperature when $T_O < 400°C$. Conceivably, a new species PtO_2 was produced on the surface of supported platinum crystallites

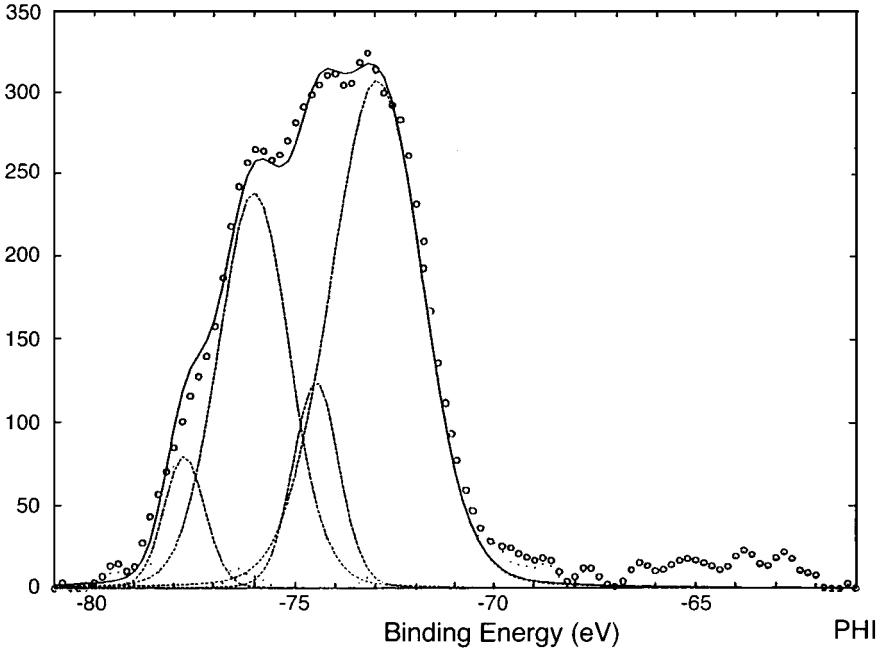

FIG. 3. XPS spectrum of Pt 4*f* signal for 4.9% Pt/SiO_2 sample oxidized at $T_0 = 400°C$.

through an extended oxidation reaction:

$$Pt^sO + 1/2\,O_2 \rightarrow Pt^sO_2. \quad [6]$$

Although PtO_2 has been found as the major platinum species on Pt/Al_2O_3 samples oxidized at 400°C (21), formation of this species on Pt/SiO_2 samples has never been confirmed in literature. The 4.9% Pt/SiO_2 sample oxidized at $T_O = 400°C$ was therefore examined by XPS spectroscopy (Fig. 3). Interestingly, besides the PtO signals (Pt 4*f* binding energy of 73.1 and 76.4 eV), signals for PtO_2 (74.6 and 77.9 eV) were also observed. The relative intensity (7 to 3) of their signals is in good agreement with the molar ratio of PtO to PtO_2 determined by TPR for the oxidized sample (Table 2).

A decrease in the N_O/N_{Pt} ratio was found in Table 2 on raising T_O temperature above 400°C. The decrease in stoichiometry of PtO_x at high oxidation temperatures may be resulted by either a decomposition of Pt^sO_2 (21), i.e.,

$$Pt^sO_2 \rightarrow Pt + O_2, \quad [7]$$

or a sublimation of Pt^sO_2 (Reaction [1]). The ICP-MS analysis for platinum loadings (Table 2) confirmed the sublimation process at $T_O > 400°C$. It is noteworthy that a sublimation of $PtO_{2(g)}$ has also been observed on Pt/Al_2O_3 samples (21), although the extent of $PtO_{2(g)}$ sublimation from Pt/Al_2O_3 samples was relatively mild.

Both peaks of PtO and Pt^sO_2 reduction appeared also in the TPR traces (Fig. 4) of reoxidized 1.0% Pt/SiO_2 samples. However, the intensity of peak S_2 (Pt^sO_2 reduction) became most prominent for a 500°C oxidation (trace (c) of Fig. 4) in contrast to the result discussed above for the higher loaded 4.9% Pt/SiO_2 sample. Probably, highly dispersed platinum particles on a lowly loaded Pt/SiO_2 sample are easier to

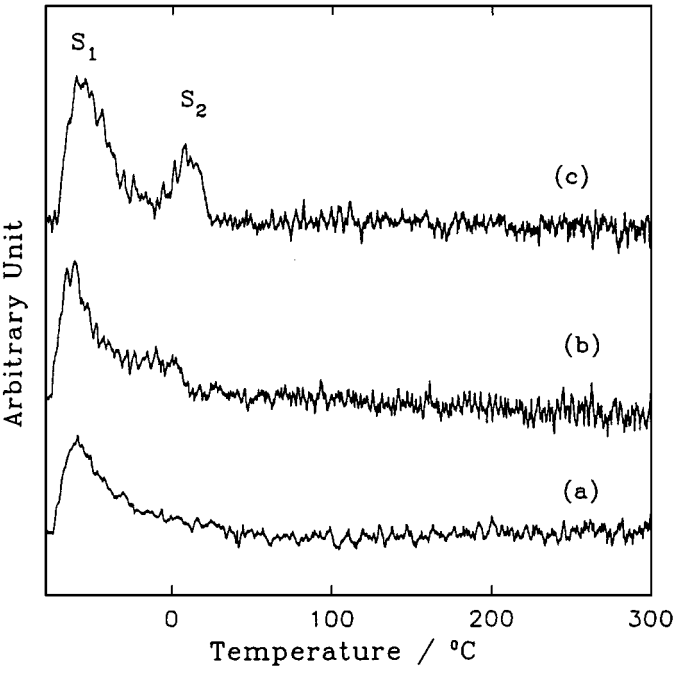

FIG. 4. TPR spectra of oxidized 1.0% Pt/SiO_2 samples which have been pretreated with a 2-h reduction in a flowing hydrogen at 300°C and a subsequent oxidation with 5% oxygen in He at $T_0 =$ (a) 25°C, (b) 300°C, and (c) 500°C.

convert into $Pt^{s}O_2$ upon a 500°C oxidation. Similar particle size effects have also been previously found from oxidations of Pt/Al_2O_3 samples (21, 24).

Table 3 summarizes TPR characterizations made in this study and a previous report (21) for different platinum species dispersed on SiO_2 and Al_2O_3 supports. Observed T_r temperatures vary significantly with chemical environments, i.e., the oxidation state and the dispersing support. Platinum species dispersed on SiO_2 supports generally exhibit lower T_r temperatures than those dispersed on Al_2O_3 supports. Observed differences in the reduction behavior of platinum species probably arise from variations in the extent of metal–support interactions.

Upon oxidation treatments at $T_O \geq 400$°C, vaporized platinum oxides were found to diffuse into the sublayers of alumina supports to form a $PtAl_2O_4$ spinal structure (21). The corresponding reduction of platinum silicate at $T_r \sim 500$°C (32) was absent in TPR traces of Pt/SiO_2 samples even when severely oxidized at $T_O \geq 400$°C. Observed substantial sublimation of $PtO_{2(g)}$ from Pt/SiO_2 samples, on comparing with Pt/Al_2O_3 (21), at $T_O \geq 400$°C (reaction [1]) should be a consequence of the low affinity between platinum and the silica support.

3.3. *Effects of Oxidation Temperature on Pt/SA-40 Samples*

Figure 5 shows TPR traces from different portions of a reduced Pt/SA-40 sample (its silica–alumina support has a SiO_2/Al_2O_3 weight ratio = 40/60) oxidized at different temperatures. These traces are composed mainly of six reduction peaks. They are tentatively designated as species S_1 ($T_r \sim -40$°C), S_2 ($T_r \sim 20$°C), A_1 ($T_r \sim 50$°C), A_2 ($T_r \sim 90$°C), C_1 ($T_r \sim 110$°C), and C_2 ($T_r \sim 130$°C), respectively. The existence of these six peaks suggests that Pt atoms on the oxidized Pt/SA-40 samples have at least six distinct chemical environments. According to the characterization of Table 3, two peaks at low T_r temperatures (S_1 and S_2) in Fig. 5 are very similar to the reduction peaks of PtO and PtO_2 species dispersed on Pt/SiO_2 samples. The middle two T_r peaks (A_1 and A_2) in traces (c–f) of Fig. 5 are similar to the reduction peaks of PtO and PtO_2 species dispersed on Pt/Al_2O_3 samples (21). Probably, the SA-40 support contains two kinds of domains, i.e., a silica-rich phase and an alumina-rich phase.

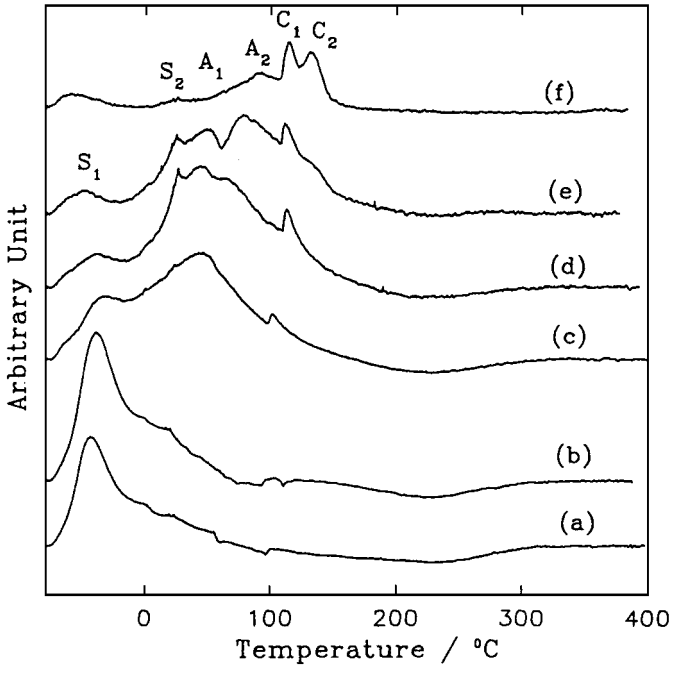

FIG. 5. TPR spectra of oxidized 4.8% Pt/SA40 samples with $T_0 =$ (a) 25°C, (b) 100°C, (c) 300°C, (d) 400°C, (e) 500°C, and (f) 600°C.

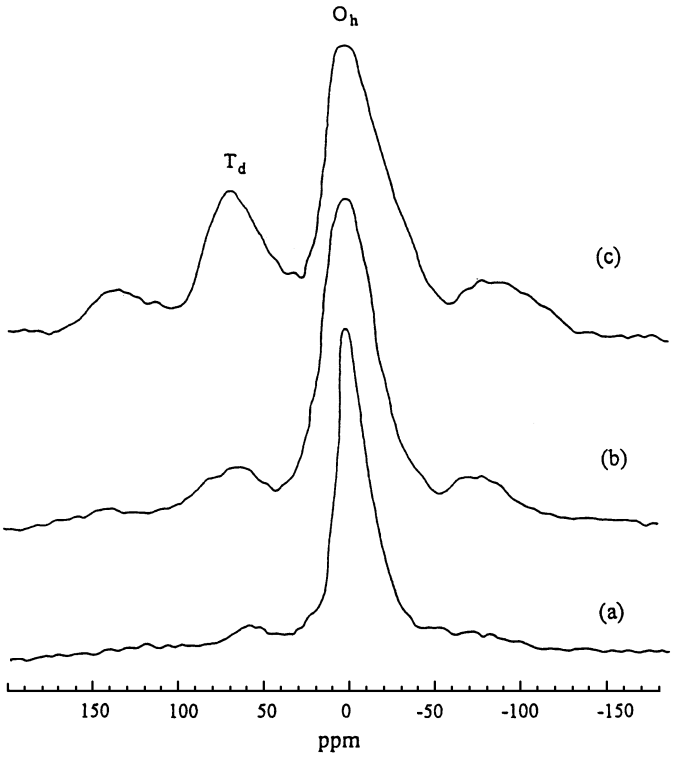

FIG. 6. Variation of ^{27}Al NMR spectra with the composition of silica-alumina supports. (a) SA80, (b) SA75, (c) SA40.

Figure 6 shows ^{27}Al NMR spectra for a series of silica–alumina supports. These spectra contained two peaks with chemical shift of $\delta = 0$ and 50 ppm. They are assigned to aluminum ions in octahedral (O_h) and tetrahedral (T_d) structures, respectively. Minor side bands are also noticed because the rate (~3000 Hz) of magic angle spin during the signal accumulation was not high enough. Trace (a) of Fig. 6 for SA-80 support (with a SiO_2/Al_2O_3 weight ratio = 80/20) exhibits a single peak with chemical shift at $\delta = 0$ ppm. Obviously, most aluminum ions in this silica–alumina support

aggregated themselves as alumina and interacted negligibly with the SiO_2 components. In other words, the silica–alumina support was indeed constituted mainly by two phases, i.e., silica-rich grains and alumina-rich grains. Evidently, the S_1 and S_2 peaks in Fig. 5 indicate that some of impregnated Pt stayed on the silica-rich grains and formed PtO and PtO_2 species during oxidation processes. The A_1 and A_2 peaks in Fig. 5 should come from reductions of PtO and PtO_2 species residing on the alumina-rich grains of the support.

A minor T_d peak ($\delta = 50$ ppm) became prominent in traces (b) and (c) of Fig. 6 as the SiO_2/Al_2O_3 ratio of SiO_2–Al_2O_3 supports was decreased. The appearance of the T_d peak indicates that a small fraction of aluminum ions in the support mixed intimately with SiO_2 components. Garofalini *et al.* (33) have verified in a computer-simulation study that cage structures were formed in the interface regions between silica-rich grains and alumina-rich grains during sol–gel preparations of silica–alumina. The T_d peak in trace (c) of Fig. 6 may be attributed to a formation of short ranged zeolite structure at the SiO_2–Al_2O_3 grain boundaries of the SA-40 support.

The appearance of species C_1 and C_2 ($T_r = 110$ and 130°C, respectively) in Fig. 5 suggests that the chemical environments of some Pt species are rather different from those dispersed on either pure SiO_2 or Al_2O_3 support. Based on TPR characterizations, both Sachtler *et al.* (25, 34) and Foger *et al.* (35) demonstrated that platinum ions in the supercage of *Y* zeolite and in the channel of *L* zeolite have T_r temperatures around 100–150°C. Based on the NMR results, both C_1 and C_2 peaks in Fig. 5 could come from reductions of Pt cations residing in pores of the zeolite structures at SiO_2–Al_2O_3 grain boundaries. These two peaks probably reflect reductions of platinum ion with two different oxidation states.

3.4. *Influence of SiO_2–Al_2O_3 Support Composition on the Distribution of Pt Species*

^{27}Al NMR spectra in Fig. 6 show that the T_d peak gradually disappeared with increasing the SiO_2/Al_2O_3 ratios of the SiO_2–Al_2O_3 supports (from SA-40, SA-75, to SA-80). The reduction of the T_d peak reveals that the formation of zeolite pores at SiO_2–Al_2O_3 grain boundaries becomes negligible and that silica-rich grains and alumina-rich grains become dominant in the samples with high Si content.

Figure 7 compares the TPR traces from different Pt/SA samples (supports with SiO_2/Al_2O_3 weight ratio = 0, 40/60, 75/25, 80/20, and ∞, respectively) oxidized at $T_O = 500$°C to study the effect of support composition. Observed changes of the TPR traces in Fig. 7 indicate variations in the distribution of different platinum species with the support composition. Peaks of S_1 and S_2 (PtO and PtO_2 on silica-rich grains) were favored on a Pt/SA-80 sample. However, the intensities of these two signals were gradually decreased and replaced by the A_1 and the A_2 signals (PtO and PtO_2 on alumina-rich grains) as the Al_2O_3/SiO_2 ratio of the support was increased. Evidently, SiO_2 and SA-80 supports lead to a formation of species S_1 and S_2, while Al_2O_3 and SA-40 supports promotes a formation of species A_1 and A_2. On the SA-40 support (with a near equilateral SiO_2/Al_2O_3 weight ratio), an appreciative fraction of platinum atoms tend to spread into the cage structures.

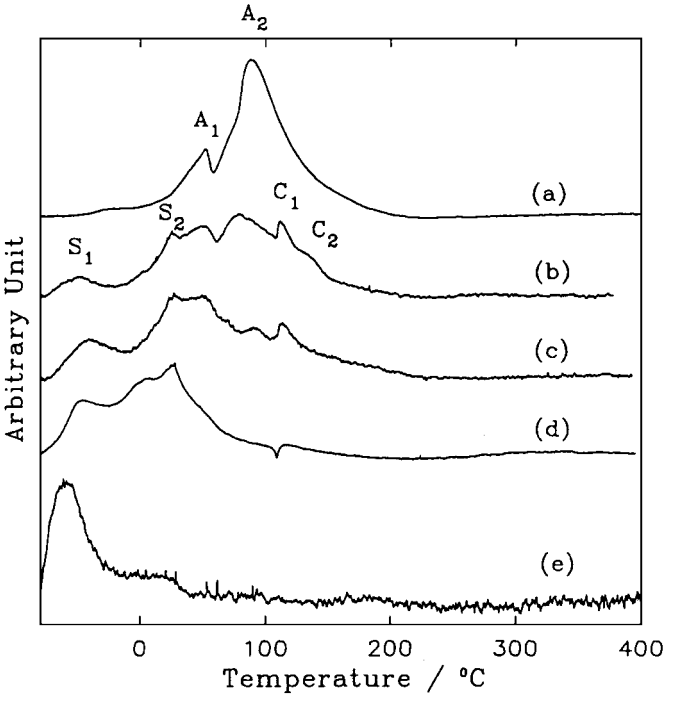

FIG. 7. A comparison of TPR spectra from different supported platinum samples oxidized at $T_0 = 500$°C. (a) 5.0% Pt/Al_2O_3, (b) 4.8% Pt/SA40, (c) 4.9% Pt/SA75, (d) 4.8% Pt/SA80, (e) 4.9% Pt/SiO_2.

4. CONCLUSIONS

Through a combination of XPS characterization, TPR study, and ICP determination, both PtO and PtO_2 species has been verified to coexist on silica supports. The ratio of PtO_2/PtO on Pt/SiO_2 samples varied with the dispersion of platinum crystallites as well as the oxidation temperature. The PtO_2 dispersed on SiO_2 support is unstable under severe oxidation environment (at $T_O \geq 400$°C) and tends to sublime into $PtO_{2(g)}$ vapor (reaction [1]). In addition, platinum-oxide species of six different chemical environments were distinguished from the Pt/SA samples. They were assigned to PtO and PtO_2 dispersed on silica-rich grains (with $T_r = -40$ and 20°C), on alumina-rich grains (with $T_r = 50$ and 90°C), and in cages at grain boundaries (with T_r about 110–130°C), respectively.

ACKNOWLEDGMENTS

The authors thank the National Science Council of Republic of China and the Chinese Petroleum Corporation for financial support of this study.

REFERENCES

1. Volter, J., Lietz, G., Spindler, H., and Lieske, H., *J. Catal.* **104**, 375 (1987).
2. Niwa, M., Awano, K., and Murakami, Y., *Appl. Catal.* **7**, 317 (1983).
3. Trimm, D. L., *Appl. Catal.* **7**, 249 (1983).
4. Vayenas, C. G., and Michaels, J. M., *Surf. Sci.* **120**, L405 (1982).
5. Vayenas, C. G., Georgakis, C., Michaels, J. M., and Tormo, J., *J. Catal.* **67**, 348 (1981).
6. Wu, N. L., and Phillips, J., *J. Catal.* **113**, 129 (1988).
7. Lieske, H., Lietz, G., Spindler, H., and Volter, J., *J. Catal.* **112**, 295 (1986).
8. Harris, P. J. F., *J. Catal.* **97**, 527 (1986).
9. Rothschild, W. G., Yao, H. C., and Plummer, H. K., Jr., *Langmuir* **2**, 588 (1986).
10. Lagarde, P., Murata, T., Vlaic, G., Freund, E., Dexpert, H., and Bournonville, J. P., *J. Catal.* **84**, 333 (1983).
11. Smith, D. J., White, D., Brird, T., and Fryer, J. R., *J. Catal.* **81**, 107 (1983).
12. Harris, P. J. F., *Surf. Sci.* **185**, L459 (1987).
13. Georgopoulos, P., and Cohen, J. B., *J. Catal.* **92**, 211 (1985).
14. Bond, G. C., and Gelsthorpe, M. R., *Appl. Catal.* **35**, 169 (1987).
15. Lieske, H., Lietz, G., Spindler, H., and Volter, J., *J. Catal.* **81**, 8 (1983).
16. Mills, G. A., Weller, S., and Cornelius, E. B., "Actes du Zieme Congr. Intern. de Catalyst," Vol. 2. Paris, 1962 (Technip, Paris, 1962).
17. McNicol, B. D., *J. Catal.* **46**, 438 (1977).
18. Yao, H. C., Sieg, M., and Plummer, H. K., Jr., *J. Catal.* **59**, 365 (1979).
19. Wagstaff, N., and Prins, R., *J. Catal.* **59**, 434 (1979).
20. Otter, G. J. D., and Dautzenberg, F. M., *J. Catal.* **53**, 116 (1978).
21. Hwang, C. P., and Yeh, C. T., *J. Mol. Catal.* **112**, 295 (1996).
22. Brewer, L., *Chem. Rev.* **52**, 1 (1953).
23. Cahen, D., Ibers, J. A., and Wagner, J. B., *Inorg. Chem.* **13**, 6 (1974).
24. Maccabe, R. W., Wong, C., and Woo, H. S., *J. Catal.* **114**, 354 (1988).
25. Park, S. H., Tzou, M. S., and Sachtler, W. M. H., *Appl. Catal.* **24**, 85 (1986).
26. Rajagopal, S., Marini, H. J., Marzari, J. A., and Miranda, R., *J. Catal.* **147**, 417 (1994).
27. Brito, J., and Laine, J., *Polyhedron* **5**, 179 (1986).
28. Wynblatt, P., and Gjostein, N. A., *Acta Metall.* **24**, 1165 (1976).
29. Chou, T. Y., Hwang, C. P., and Yeh, C. T., *J. Thermal Anal.* **46**, 305 (1996).
30. Masayoshi, K., Yasunobn, I., Nobuo, T., Robert, L. B., John, B. B., and Jerome, B. C., *J. Catal.* **64**, 74 (1980).
31. Mullinberg, G. E., "Handbook of X-ray Photoelectron Spectroscopy." Perkin-Elmer Corp., Physical Electrics Division, Eden Prairie, MN, 1987.
32. Ho, L. W., Hwang, C. P., Lee, J. F., Wang, I. K., and Yeh, C. T., *J. Mol. Catal.*, in press.
33. Blonski, S., and Garofalini, S. H., *J. Phys. Chem.* **100**, 2201 (1996).
34. Ostgard, D. J., Kustov, L., Poeppelmeier, K. R., and Sachtler, W. M. H., *J. Catal.* **133**, 342 (1992).
35. Foger, K., and Jaeger, H., *Appl. Catal.* **56**, 137 (1989).